Intense harmonics generation with customized photon frequency and optical vortex

2016 New J. Phys. 18 083046

(http://iopscience.iop.org/1367-2630/18/8/083046)

New Journal of Physics
The open access journal at the forefront of physics

Deutsche Physikalische Gesellschaft DPG
IOP Institute of Physics

Published in partnership with: Deutsche Physikalische Gesellschaft and the Institute of Physics

OPEN ACCESS

RECEIVED
11 May 2016

REVISED
30 July 2016

ACCEPTED FOR PUBLICATION
5 August 2016

PUBLISHED
24 August 2016

PAPER

Intense harmonics generation with customized photon frequency and optical vortex

Xiaomei Zhang[1,2], Baifei Shen[1,3], Yin Shi[1], Lingang Zhang[1], Liangliang Ji[4], Xiaofeng Wang[1], Zhizhan Xu[1] and Toshiki Tajima[2]

[1] State Key Laboratory of High Field Laser Physics, Shanghai Institute of Optics and Fine Mechanics, Chinese Academy of Sciences, Shanghai 201800, People's Republic of China
[2] University of California, Irvine, 92697 USA
[3] IFSA Collaborative Innovation Center, Shanghai Jiao Tong University, Shanghai 200240, People's Republic of China
[4] Department of Physics, The Ohio State University, Columbus, Ohio 43210, USA

E-mail: zhxm@siom.ac.cn **and** bfshen@mail.shcnc.ac.cn

Keywords: intense vortex beam, high harmonics generation, tunable

Abstract

An optical vortex with orbital angular momentum (OAM) enriches the light and matter interaction process, and helps reveal unexpected information in relativistic nonlinear optics. A scheme is proposed for the first time to explore the origin of photons in the generated harmonics, and produce relativistic intense harmonics with expected frequency and an optical vortex. When two counter-propagating Laguerre–Gaussian laser pulses impinge on a solid thin foil and interact with each other, the contribution of each input pulse in producing harmonics can be distinguished with the help of angular momentum conservation of photons, which is almost impossible for harmonic generation without an optical vortex. The generation of tunable, intense vortex harmonics with different photon topological charge is predicted based on the theoretical analysis and three-dimensional particle-in-cell simulations. Inheriting the properties of OAM and harmonics, the obtained intense vortex beam can be applied in a wide range of fields, including atom or molecule control and manipulation.

1. Introduction

The vortex beam exhibiting a helical wavefront can be applied as a powerful probing tool in studying cold atoms, atomic transition [1–7], design and operation of micromachines [8], optical communications and quantum space [9–11] and even astrophysics [12]. Such a beam can even transfer orbital angular momentum (OAM) to material particles, rotate them, or manipulate their vortex characteristics when the intensity is sufficiently high. Recent researches have proved its possible usage in particle acceleration [13], and the vortex beams can be amplified and generated to petawatt intensities in plasmas through stimulated Raman backscattering [14]. The helical characteristic of a vortex beam is described by the phase component of $\exp(il\phi)$, where ϕ is the azimuthal coordinate and the integer number l is the topological charge [15–17]. Different values of l mean that the photon has different vortex characteristics and carries different OAMs. Owing to the limitation of the etching resolution, it is difficult to obtain a vortex beam of high topological charge through conventional methods such as forked diffraction gratings [18, 19] or spiral phase plates [15]. There have been some efforts, such as the use of a helical undulator [20–22], Compton backscattering effects [23, 24], and high-order harmonics generation (HHG) [25–28], devoted to generating a light beam with OAM. Among them, the HHG scheme has an extraordinarily promising perspective because of the confluence of OAM and HHG, and experimental results have been demonstrated [26, 28]. In the previous HHG scheme, one incident pulse is used, and only certain topological charges of the HHG are generated and cannot be tuned. Thus, the application will be inevitably limited to some extent when a light beam with a specific OAM and frequency is required.

In this paper, we present a new way to generate ***tunable*** intense vortex beams of high topological charge from laser-plasma interactions, in which the frequency and mode of the radiation harmonics can be tuned to meet

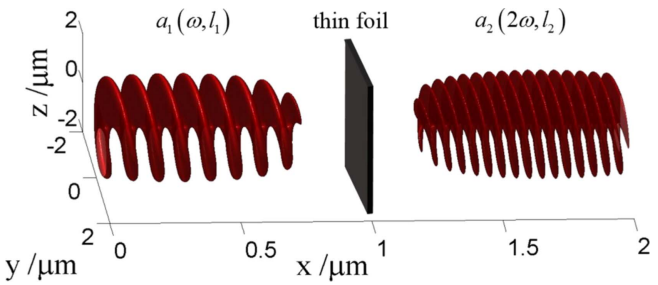

Figure 1. Schematic of the proposed scheme. Two counter-propagating CPLG laser pulses a_1 and a_2 with frequencies and orders of $(n_1\omega, l_1)$ and $(n_2\omega, l_2)$, respectively, irradiate on a thin foil ($n_1 = 1, l_1 = 1, n_2 = 2$, and $l_2 = 2$).

different requirements. More importantly, this is the first attempt to determine the origin of photons of the generated harmonics through the coupling process of high harmonics. In this scheme, two counter-propagating intense driving vortex beams with low topological charges impinge on a thin foil. Due to their interaction in the foil, high-order harmonics are radiated on both sides. With the help of a photon vortex, the contribution of input pulses in producing harmonics can be distinguished. The topological charge and order of harmonics can be designed by adjusting the parameters of the input pulses, which promises more possibilities with an additional pulse compared with the case of a single driving pulse.

Compared with the well-known gas HHG sources, the present scheme is in the relativistic ($>10^{18}$ W cm^{-2}) laser plasma interaction range. Using plasma as the mode-converter, the intensity of the vortex beam can be increased by several orders of magnitude compared with that of the gas HHG scheme, in which it is impossible to generate such an intense vortex beam because of the limitations (often below 10^{15-16} W cm^{-2}) of the laser intensity to avoid strong ionization. The generation mechanism in the present scheme is independent of the input laser polarization state, which is different from that in our previous study, in which the high order vortex beam is obtained from the oscillating foil surface by using a linearly polarized laser pulse [27]. Here, the high harmonics with large OAM are radiated from the oscillating electrons, which are well confined by the two pulses, and most importantly, the two laser pulses allow better flexibility in the sense of generating OAM. The mode can be tuned by adjusting the driving pulses individually, thereby satisfying different requirements.

2. Theoretical analysis

The proposed scheme is shown in figure 1. Two counter-propagating circularly polarized (CP) Laguerre–Gaussian (LG) laser pulses a_1 and a_2 with the same rotation directions (both left handed or right handed CP) with frequencies and topological charges of $(n_1\omega, l_1)$ and $(n_2\omega, l_2)$, respectively, irradiate on a thin foil. For this scheme, electrons are pushed inside from both sides of the foil and are well confined within the foil by the radiation pressure. High harmonics are generated from the oscillating electrons. The foil is thinner than the skin depth to ensure full interaction of the two pulses inside the target. This is not the first time HHG have been produced with two pulses [29, 30], however, LG pulses bring the high topological charge of harmonics, which is our main focus. To overcome the drawback of the limited multiplication factor with a single frequency conversion, the use of beam-echo effect induced by an additional laser beam has been found more efficiently in the HHG generation [31, 32]. Here with the similar motivation, the main focus is that the high topological charge concerning to the large OAM can be tunable. The normalized vector potential ($a = eA/m_e c^2$, where A is the vector potential, c is the light speed in vacuum, m_e is the electron mass, and e is the electron charge) of the laser amplitude inside of the electron layer can be written as

$$\begin{aligned} a &= a_1 + a_2 \\ &= 2a_0 \begin{bmatrix} \cos(((n_2 - n_1)\omega t + (l_2 - l_1)\phi)/2)\hat{x} \\ + \sin(((n_2 - n_1)\omega t + (l_2 - l_1)\phi)/2)\hat{y} \end{bmatrix} \sin(((n_2 + n_1)\omega t + (l_2 + l_1)\phi)/2), \end{aligned}$$

where a_1 and a_2 are used as

$$\begin{aligned} a_1 &= a_0[\sin(n_1\omega t + l_1\phi)\hat{x} + \cos(n_1\omega t + l_1\phi)\hat{y}], \\ a_2 &= a_0[\sin(n_2\omega t + l_2\phi)\hat{x} - \cos(n_2\omega t + l_2\phi)\hat{y}] \end{aligned}$$

for simplicity, since only phase terms are concerned, where a_0 is the normalized vector potential. The electron transverse velocity is $\nu = a/\gamma$, which is the source term and contributes to the nonlinearity in Maxwell's equation

$$\nabla^2 a - \partial^2 a/\partial t^2 = nv,$$

where $\gamma = (1 + a^2)^{1/2}$ is the relativistic factor, v is normalized to the light speed c and n is the electron density. We only analyze the source term to interpret the dominant source of harmonics generation and the corresponding phase terms which originates from the electron movement under the field inside the foil, rather than an exact solution for all physical variables. From the Fourier expansion of this source term, we can see that it contains the following components:

$$\begin{bmatrix} \sin(n_{m1}\omega t + l_{m1}\phi)\hat{x} + \cos(n_{m1}\omega t + l_{m1}\phi)\hat{y} \\ \sin(n_{m2}\omega t + l_{m2}\phi)\hat{x} - \cos(n_{m2}\omega t + l_{m2}\phi)\hat{y} \end{bmatrix}, \tag{1}$$

where $n_{\mathrm{m1(2)}}$ and $l_{\mathrm{m1(2)}}$ are the order and topological charge of generated harmonics and

$$\begin{aligned} n_{m1} &= ((m+1)n_1 + mn_2),\ l_{m1} = ((m+1)l_1 + ml_2); \\ n_{m2} &= (mn_1 + (m+1)n_2),\ l_{m2} = (ml_1 + (m+1)l_2), \end{aligned} \tag{2}$$

and $m = 0, 1, 2, \ldots$. From equation (1), two kinds of harmonics carrying the frequency and OAM information of the input pulses are generated, i.e., the n_{m1} order harmonics with a topological charge of l_{m1} and the n_{m2} order harmonics with a topological charge of l_{m2} can be obtained with this regime. Based on this, it can be concluded that a vortex beam with a specific topological charge and frequency can be obtained by combining the four given variables n_1, n_2, l_1, l_2 to meet different requirements.

Considering photons in the nonlinear process of the present scheme, for the n_{m1} order harmonic, each photon carries an energy $n_{\mathrm{m1}}\hbar\omega$. For the input pulses without helicity, it is difficult to distinguish where the generated harmonic photons originate from or how many photons of pulse a_1 and a_2 are consumed in the nonlinear process. This is because the photons of two pulses cannot be distinguished completely just according to the energy conservation depending solely on the photon frequency. That is, one cannot determine the exact values of X, Y just from $Xn_1\hbar\omega + Yn_2\hbar\omega = n_{m1}\hbar\omega$, where X, Y are the photon numbers from pulse a_1 and pulse a_2. However, when the photons of the input pulses have vortex properties, i.e., the OAM in the present scheme, there is an additional freedom degree l. According to the OAM conservation $Xl_1\hbar + Yl_2\hbar = n_{m1}\hbar$, we can easily deduce that one photon of the n_{m1} order harmonic is transformed from $(m+1)$ photons of pulse a_1 and (m) photons of pulse a_2. Similarly, one photon of the n_{m2} order harmonic is transformed from (m) photons of pulse a_1 and $(m+1)$ photons of pulse a_2. It is same with the sum frequency generation in nonlinear optics. From equation (1), it can be seen that the harmonics of n_{m1} and n_{m2} order maintain the same rotation direction as pulse a_1 and a_2, respectively, which means all helicities of photons including spin (polarization) [33] and orbit are conserved in this nonlinear HHG process. Using the helicity of the optical vortex in the present scheme, apart from the generation of the tunable, intense high-order optical vortex beam, we can determine the process that the photons undergo during the generation of different order harmonics, which is helpful to understand this nonlinear process in plasma.

3. Three-dimensional PIC simulations

To confirm the above analysis, three-dimensional (3D) particle in cell (PIC) simulations have been performed. We carried out all simulations using EPOCH code [34]. The driving LG beam is described as

$$a(LG_{lp}) = a_0 \left(\frac{\sqrt{2}\,r}{r_0}\right)^l \exp\left(-\frac{r^2}{r_0^2}\right) \exp(il\phi) \exp(i\omega t)(-1)^p L_p^l\left(\frac{2r^2}{r_0^2}\right) \sin^2\left(\frac{\pi t}{2t_0}\right).$$

The left pulse a_1 has a frequency of ω corresponding to the wavelength of $\lambda = 1\ \mu$m and the right pulse a_2 has frequency of 2ω corresponding to the wavelength of $\lambda/2 = 0.5\ \mu$m. $r_0 = 6\ \mu$m, and $t_0 = 5T$ are used for the two pulses, where T is the left driving laser period. The topological charges of the a_1 and a_2 pulses are l_1 and l_2, respectively. For the left pulse, laser wavelength of $\lambda = 1\ \mu$m, $a_0 = 5$ corresponds to a peak electric field intensity of 9.6×10^{12} V m^{-1}. The same peak electric field for the right laser pulse is used. The thin foil with the thickness of $0.1\ \mu$m as the nonlinear converter occupies the region $9.95\ \mu\mathrm{m} < x < 10.05\ \mu$m in the propagation direction of the driving beam and $-13.5\ \mu\mathrm{m} < y(z) < 13.5\ \mu$m in the transverse direction with a density of $n_0 = 20n_c$, where $n_c = 1.1 \times 10^{21}$ cm^{-3} is the critical density for the left laser pulse. The simulation box is $20\ \mu\mathrm{m}\,(x) \times 30\ \mu\mathrm{m}\,(y) \times 30\ \mu\mathrm{m}\,(z)$, and corresponds to a window with $1000 \times 400 \times 400$ cells and 100 particles per cell for the foil. At $t = 0$, the laser pulses enter the simulation box from both boundaries.

The isosurface distribution of the laser electric field and the thin foil density in this simulation are shown in figure 1. Figure 2 shows the frequency spectrum of the whole laser field including the reflected and transmission parts, which shows that each third harmonic (3th, 6th, …) is missing. Here we note the amplitude of twin harmonics (1st & 2nd, 4th & 5th, and 7th & 8th) are almost equal because of the same intensity of the both pulses a_1 and a_2. According to equation (2), for $n_1 = 1, n_2 = 2$, the frequency spectrum of the generated harmonics

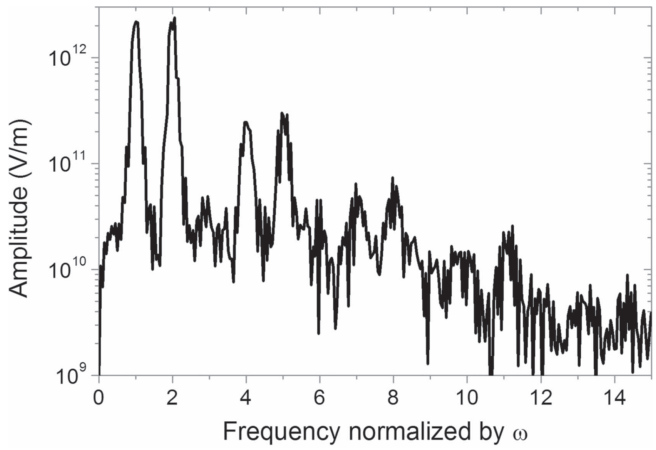

Figure 2. Frequency spectrum of the laser field after interaction between the input pulses and thin foil. The field signal at $y = 5$ μm and $z = 0$ μm is used. The peak electric field intensity is 9.6×10^{12} V m^{-1} for both input pulses.

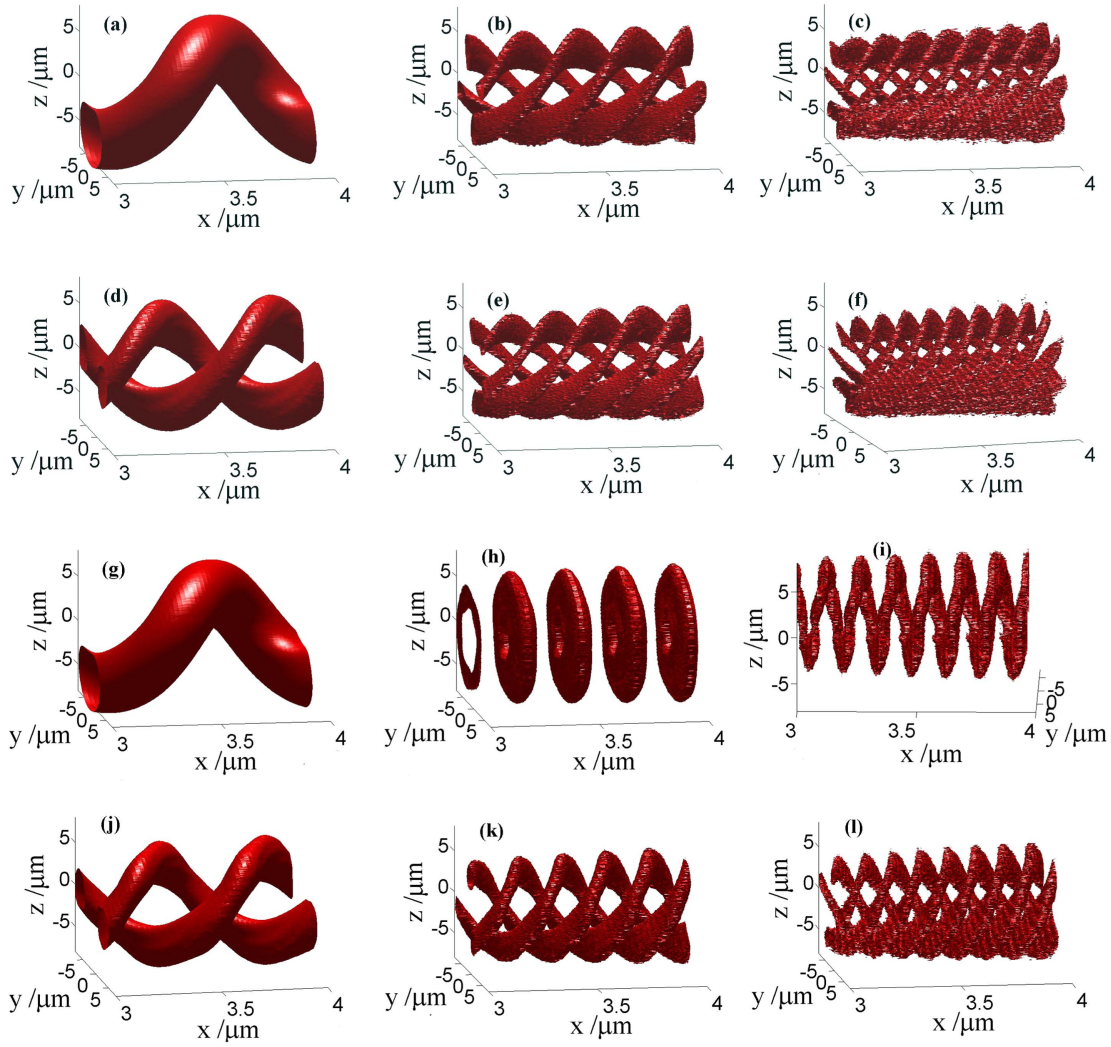

Figure 3. Electric field isosurface of the (a), (g) first, (d), (j) second, (b), (h) fourth, (e), (k) fifth, (c), (i) seventh, and (f), (l) eighth harmonics within a 1 μm distance in the propagating direction after the interaction in the case of (a)–(f) $l_1 = 1, l_2 = 2$ and (g)–(l) $l_1 = -1, l_2 = 2$.

only contains $(3m + 1)\omega$ and $(3m + 2)\omega$, which well explains the spectrum in the simulation. Most importantly, the corresponding topological charges of these harmonics are $(m + 1)l_1 + ml_2$ and $ml_1 + (m + 1)l_2$, which means that the topological charges of the generated harmonics 1, 2, 4, 5, 7, 8, …,

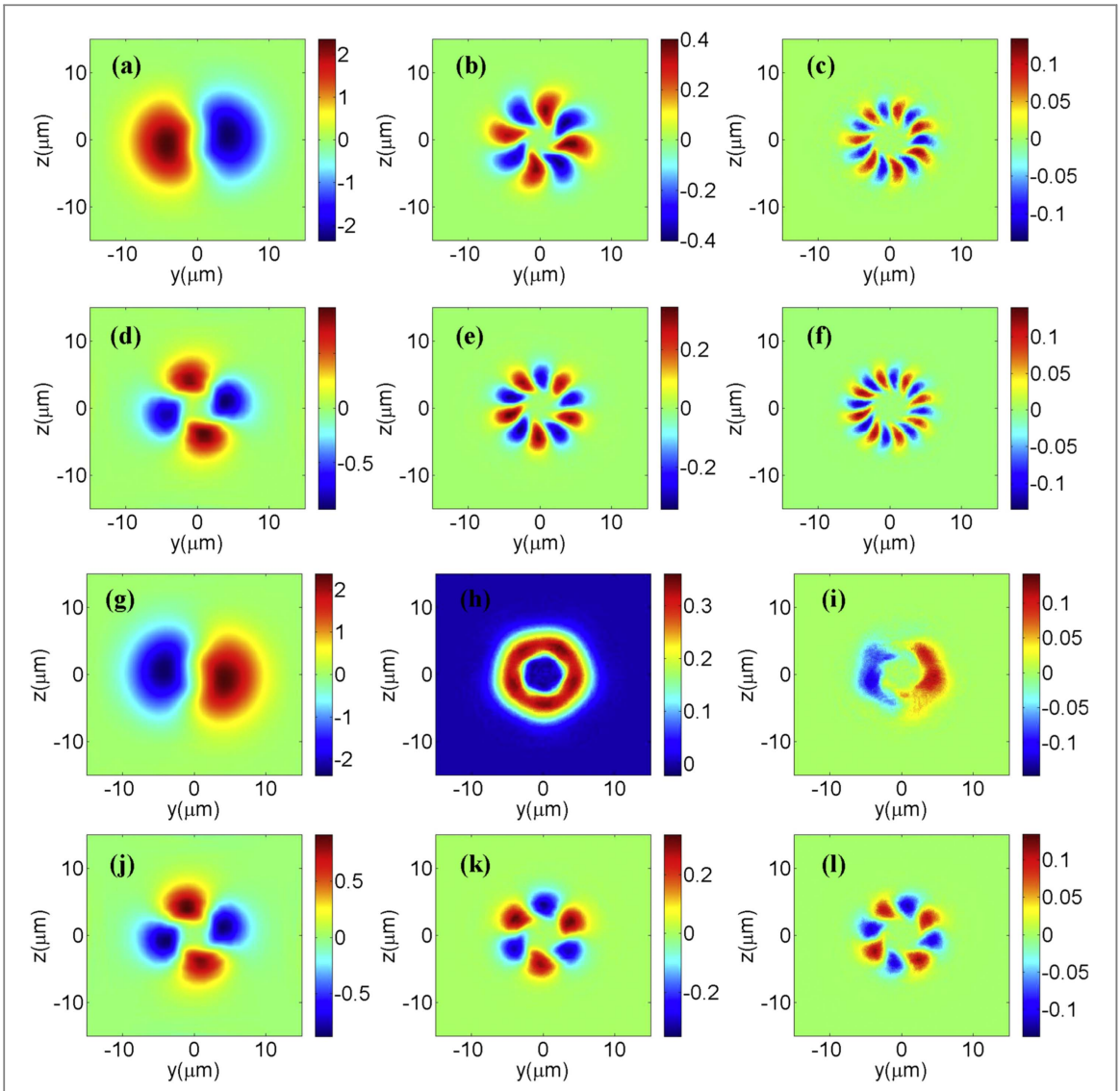

Figure 4. Electric field distribution of the (a), (g) first, (d), (j) second, (b), (h) fourth, (e), (k) fifth, (c), (i) seventh, and (f), (l) eighth harmonics in the z-y plane at $x = 4$ μm after the interaction in the case of (a)–(f) $l_1 = 1, l_2 = 2$ and (g)–(l) $l_1 = -1, l_2 = 2$. The field is normalized to $m_e\omega c/e$ (4×10^{12} V m^{-1}).

$(3m + 1), (3m + 2)$ should be $l = 1, 2, 4, 5, 7, 8, \ldots, (3m + 1), (3m + 2)$ for $l_1 = 1, l_2 = 2$, and $l = -1, 2, 0, 3, 1, 4, \ldots, (m - 1), (m + 2)$ for $l_1 = -1, l_2 = 2$. Figures 3 and 4 show the electric field isosurface of different order harmonics within one wavelength of the left pulse (1 μm) for the cases of $l_1 = 1, l_2 = 2$ and $l_1 = -1, l_2 = 2$, and the corresponding transverse electric field distribution in the same y-z plane after the laser foil interaction. From these structures in the figures, the wavelength, helicity, and topological charge of the harmonics can be seen clearly, and are in good agreement with the theoretical analysis results. For example, the clear LG_{80}-like mode is obtained, in which each photon has an OAM of $8\hbar$ and the peak electric field intensity is of 10^{11} V cm^{-1} in the case of $l_1 = 1, l_2 = 2$. It should be noted that in the case of $l_1 = -1, l_2 = 2$, the field in the center of the fourth harmonics is close to zero due to the similar intensity distribution of the both input source fields, although its topological charge is $l = 0$.

We should note that the resolution in the x direction is not enough for the high order harmonics (>10th) with the present resolution, but it is enough for the lower order harmonics. The results are in good agreement with the theoretical analysis. Actually, when the resolution is doubled, even the higher order harmonics (10th and 11th) are clearer, besides the low order ones.

4. Discussion

The normal incidence of two beams has been analyzed to show the main idea clearly. In the perspective of the experimental setup, the influence of the incident angle on the vortex beam generation should be considered.

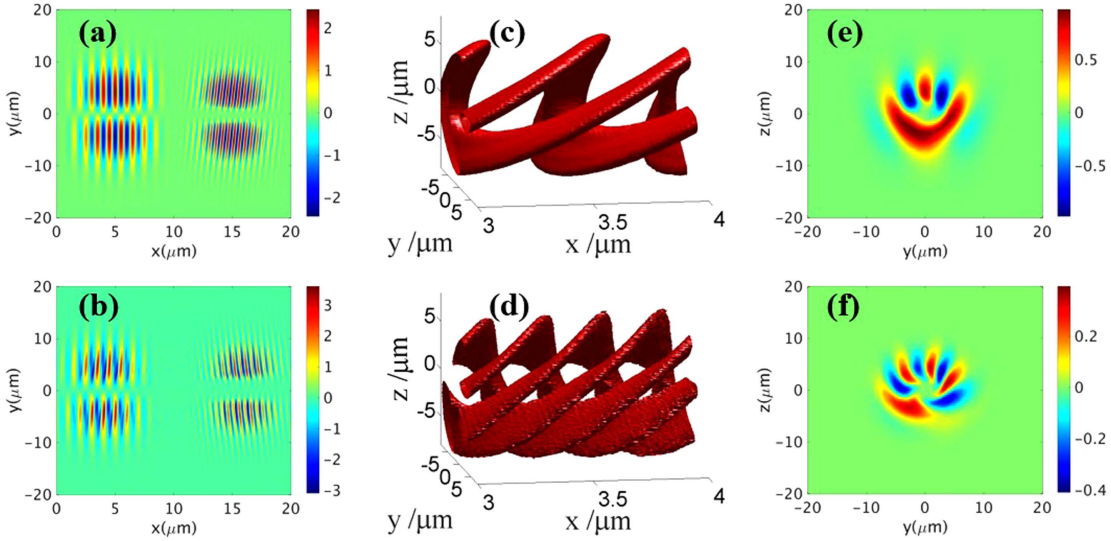

Figure 5. Electric field distribution in the y-x plane at $z = 0$ μm before (a) and after (b) the interaction between the laser pulses and thin foil in the case of $l_1 = 1, l_2 = 2$. Electric field isosurface of the (c) 2nd and (d) 4th harmonics within a 1 μm distance in the propagating direction after the interaction. Electric field distribution of the (e) 2nd and (f) 4th harmonics in the z-y plane at $x = 4$ μm after the interaction. The field is normalized to $m_e\omega c/e$ (4×10^{12} V m^{-1}) and the right laser pulse propagates at an angle of $\alpha = \pi/64$.

Figures 5(a) and (b) show the laser electric fields before and after the interaction with the thin foil when the right laser pulse irradiates obliquely with the incident angle $\alpha = \pi/64$. In this case, the electric field E_y after the interaction carries on the influence of the incident angle. Different wave fronts of a_2 cross the y-axis at different places, and this forms a sinusoidal profile with the wavelength of $\lambda/(2\sin\alpha)$ along y that represents the phase, where $\lambda/2$ is the wavelength of the laser a_2. Therefore, the k_y component (wave vector in the y direction) of a_2 in the case of oblique incidence results in the distortion of the wave fronts of the reflected beam. And the distortion grows strong with the incident angle. Considering the small influence brought by the k_y component of the incident beam, in which the field of k_y component of a_2 is weak and does not interrupt the information of harmonics along x-axis, it is better to drive the beam at a small angle. In this case, the harmonics and their corresponding topological charge keep almost the same with the results of the normal incidence case as shown in figures 5(c) and (d), except for little influence on the phase change within one loop shown in figures 5(e) and (f).

In the example above, the two driving CP pulses have the same rotation directions. In the case of the counter-rotation directions, the topological charge and order of harmonics can also be determined with the same analytical method, that is, for the $(m+1)n_{1(2)} - mn_{2(1)}$ order harmonic, the topological charge is $(m+1)l_{1(2)} - ml_{2(1)}$. For $n_1 = 1, l_1 = -1$ and $n_2 = 2, l_2 = 2$, the harmonic order and its corresponding topological charge are $1, 2, 3, 4, 5, \ldots, (m+1)$ and $-1, 2, 5, 8, 11, \ldots, (3m-1)$, which is confirmed by our simulations. Interestingly, for the counter-rotation case, one photon of the $(m+1)n_{1(2)} - mn_{2(1)}$ harmonic is transformed from $(m+1)$ photons of $a_{1(2)}$, and at the same time m photons of $a_{2(1)}$ are generated, which may be annihilated during the other order harmonics process. Different from the sum frequency generation process in the same-rotation case, this is a difference frequency generation process. In addition, CP laser pulses are used as the example to distinguish the HHG in terms of the oscillating mirror model, in which the neither of the CP lasers would produce harmonics by itself, Actually, the present scheme is effective even for linearly polarized lasers, and high harmonics with different topological charges are generated.

The vortex beam with high topological charge opens a wide range of applications, since a new freedom degree, i.e., OAM, is included. According to equation (2), the topological charge of the high order harmonics can be further increased when the vortex beams with high charge acquired with this scheme or others [14, 27, 35] are input. Large OAM can make a huge mechanical torque when it interacts with matter, and help to control and manipulate micro-particles. The circular or elliptical polarization laser pulse as a chiroptical characterization tool has been applied in probing chiral molecules during the gas HHG process [36, 37]. The generation of a much stronger and tunable infrared vortex laser provides an alternative tool with a new freedom degree. The new freedom degree will also help to understand the nonlinear physical process, such as the transformation of photons with different topological charge in the process of multiple frequency generation and sum or difference frequency generation, especially when two or more pulses are involved. Inspired by the amplification and generation of the intense twisted laser pulses via stimulated Roman scattering [14], researchers expect to find more optical-parametric-like process when such beams interact with some chiral materials.

5. Conclusion

In conclusion, a new scheme to obtain tunable intense high-order vortex beams in the high frequency region from laser plasma interaction is proposed, and it provides an approach to produce the vortex beam with a specific OAM and frequency as expected. For the first time the additional freedom degree gives us insight into the photon process and helps determine the origin of harmonics photon when two pulses are involved. Both theoretical analysis and 3D PIC simulations have confirmed the generation of high harmonics carrying large OAM when two counter-propagating intense driving vortex beams interact in a thin foil. The topological charge and order of harmonics can be predicted by adjusting the input pulses. Corresponding experimental research is expected based on the well-developed solid HHG diagnostics [38–44].

Acknowledgments

This work was supported by the National Natural Science Foundation of China (61221064, 11374319, 11125526, 11335013, 11674339 and 11127901).

References

[1] Clifford M A *et al* 1998 High-order Laguerre–Gaussian laser modes for studies of cold atoms *Opt. Commun.* **156** 300
[2] Davis B S, Kaplan L and McGuire J H 2013 On the exchange of orbital angular momentum between twisted photons and atomic electrons *J. Opt.* **15** 035403
[3] Afanasev A, Carlson C E and Mukherjee A 2013 Off-axis excitation of hydrogenlike atoms by twisted photons *Phys. Rev.* A **88** 033841
[4] Picon A *et al* 2010 Transferring orbital and spin angular momenta of light to atoms *New J. Phys.* **12** 083053
[5] Andersen M F *et al* 2006 Quantized rotation of atoms from photons with orbital angular momentum *Phys. Rev. Lett.* **97** 170406
[6] Peshkov A A *et al* 2016 Absorption of twisted light by a mesoscopic atomic target *Phys. Scr.* **91** 064001
[7] Scholz-Marggraf H M *et al* 2014 Absorption of twisted light by hydrogenlike atoms *Phys. Rev.* A **90** 013425
[8] Padgett M and Bowman R 2011 Tweezers with a twist *Nat. Photon.* **5** 343–8
[9] Wang J *et al* 2012 Terabit free-space data transmission employing orbital angular momentum multiplexing *Nat. Photon.* **6** 488–96
[10] Bozinovic N *et al* 2013 Terabit-scale orbital angular momentum mode division multiplexing in fibers *Science* **340** 1545–8
[11] Molina-Terriza G, Torres J P and Torner L 2007 Twisted photons *Nat. Phys.* **3** 305–10
[12] Tamburini F *et al* 2011 Twisting of light around rotating black holes *Nat. Phys.* **7** 195–7
[13] Vieira J and Mendonça J T 2014 Nonlinear laser driven donut wakefields for positron and electron acceleration *Phys. Rev. Lett.* **112** 215001
[14] Vieira J *et al* 2016 Amplification and generation of ultra-intense twisted laser pulses via stimulated Raman scattering *Nat. Commun.* **7** 10371
[15] Yao A M and Padgett M J 2011 Orbital angular momentum: origins, behavior and applications *Adv. Opt. Photon.* **3** 161
[16] Franke-Arnold S, Allen L and Padgett M 2008 Advances in optical angular momentum *Laser Photon. Rev.* **2** 299
[17] Allen L *et al* 1992 Orbital angular-momentum of light and the transformation of Laguerre–Gaussian laser modes *Phys. Rev.* A **45** 8185–9
[18] Bazhenov V Y, Vasnetsov M V and Soskin M S 1990 Laser-beams with screw dislocations in their wave-fronts *JETP Lett.* **52** 429
[19] Chen P *et al* 2015 Arbitrary and reconfigurable optical vortex generation: a high-efficiency technique using director-varying liquid crystal fork gratings *Photon. Res.* **3** 133–9
[20] Hemsing E *et al* 2013 Coherent optical vortices from relativistic electron beams *Nat. Phys.* **9** 549–53
[21] Hemsing E *et al* 2009 Helical electron-beam microbunching by harmonic coupling in a helical undulator *Phys. Rev. Lett.* **102** 174801
[22] Hemsing E, Marinelli A and Rosenzweig J B 2011 Generating optical orbital angular momentum in a high-gain free-electron laser at the first harmonic *Phys. Rev. Lett.* **106** 164803
[23] Jentschura U D and Serbo V G 2011 Generation of high-energy photons with large orbital angular momentum by compton backscattering *Phys. Rev. Lett.* **106** 013001
[24] Jentschura U D and Serbo V G 2011 Compton upconversion of twisted photons: backscattering of particles with non-planar wave functions *Eur. Phys. J.* C **71** 1571
[25] Hernandez-Garcia C *et al* 2013 Attosecond extreme ultraviolet vortices from high-order harmonic generation *Phys. Rev. Lett.* **111** 083602
[26] Patchkovskii S and Spanner M 2012 Nonlinear optics high harmonics with a twist *Nat. Phys.* **8** 707
[27] Zhang X M *et al* 2015 Generation of intense high-order vortex harmonics *Phys. Rev. Lett.* **114** 173901
[28] Gariepy G *et al* 2014 Creating high-harmonic beams with controlled orbital angular momentum *Phys. Rev. Lett.* **113** 153901
[29] Shen B F and Meyer-ter-Vehn J 2001 High-density (>10(23)/cm(3)) relativistic electron plasma confined between two laser pulses in a thin foil *Phys. Plasmas* **8** 1003–10
[30] Yu Y H *et al* 2013 Enhanced high harmonic generation and the phase effect in double-sided relativistic laser-foil interaction *Phys. Plasmas* **20** 033109
[31] Stupakov G 2009 Using the beam-echo effect for generation of short-wavelength radiation *Phys. Rev. Lett.* **102** 074801
[32] Hemsing E and Marinelli A 2012 Echo-enabled x-ray vortex generation *Phys. Rev. Lett.* **109** 224801
[33] Tajima T 1977 Helicity conservation in a parametric scattering instability in a magnetic-field *Phys. Fluids* **20** 61–4
[34] Arber T D *et al* 2015 Contemporary particle-in-cell approach to laser-plasma modelling *Plasma Phys. Control. Fusion* **57** 113001
[35] Shi Y *et al* 2014 Light fan driven by a relativistic laser pulse *Phys. Rev. Lett.* **112** 235001
[36] Cireasa R *et al* 2015 Probing molecular chirality on a sub-femtosecond timescale *Nat. Phys.* **11** 654–8
[37] Cho M 2015 High-harmonic generation: drive round the twist *Nat. Phys.* **11** 621–2

[38] Bulanov S V, Naumova N M and Pegoraro F 1994 Interaction of an ultrashort, relativistically strong laser-pulse with an overdense plasma *Phys. Plasmas* **1** 745
[39] Lichters R, MeyerterVehn J and Pukhov A 1996 Short-pulse laser harmonics from oscillating plasma surfaces driven at relativistic intensity *Phys. Plasmas* **3** 3425
[40] Gordienko S *et al* 2004 Relativistic doppler effect: universal spectra and zeptosecond pulses *Phys. Rev. Lett.* **93** 115002
[41] Baeva T, Gordienko S and Pukhov A 2006 Theory of high-order harmonic generation in relativistic laser interaction with overdense plasma *Phys. Rev.* E **74** 046404
[42] Teubner U and Gibbon P 2009 High-order harmonics from laser-irradiated plasma surfaces *Rev. Mod. Phys.* **81** 445
[43] Dromey B *et al* 2006 High harmonic generation in the relativistic limit *Nat. Phys.* **2** 456
[44] Naumova N M, Nees J A and Mourou G A 2005 Relativistic attosecond physics *Phys. Plasmas* **12** 056707